Gallic acid suppresses the progression of clear cell renal cell carcinoma through inducing autophagy via the PI3K/Akt/Atg16L1 signaling pathway

TIANXIANG ZHANG[1,2], XI ZHANG[3], YANG FEI[2], JINSEN LU[4], DAIRAN ZHOU[5], LI ZHANG[1,6,7], SONG FAN[1,6,7], JUN ZHOU[1,6,7], CHAOZHAO LIANG[1,6,7] and YANG SU[1,6,7]

[1]Department of Urology, The First Affiliated Hospital of Anhui Medical University, Hefei, Anhui 230032; [2]State Key Laboratory of Systems Medicine for Cancer, Department of Urology, Shanghai Cancer Institute, Ren Ji Hospital, Shanghai Jiao Tong University School of Medicine, Shanghai 200127; [3]Department of Urology, The Second Hospital of Shanxi Medical University, Taiyuan, Shanxi 030001, P.R. China; [4]Nuffield Department of Orthopedics, Rheumatology and Musculoskeletal Sciences, University of Oxford, Oxford OX3 7LD, UK; [5]Department of Neurosurgery, Changzheng Hospital, Naval Medical University, Shanghai 200003; [6]Institute of Urology, Anhui Medical University, Hefei, Anhui 230032; [7]Anhui Province Key Laboratory of Urological and Andrological Diseases Research and Medical Transformation, Hefei, Anhui 230032, P.R. China

Received June 10, 2023; Accepted November 22, 2023

DOI: 10.3892/ijo.2024.5658

Abstract. Clear cell renal cell carcinoma (ccRCC), the most common type of renal cell carcinoma (RCC), is not sensitive to traditional radiotherapy and chemotherapy. The polyphenolic compound Gallic acid (GA) can be naturally found in a variety of fruits, vegetables and plants. Autophagy, an intracellular catabolic process, regulates the lysosomal degradation of organelles and portions in cytoplasm. It was reported that autophagy and GA could affect the development of several cancers. Therefore, the aim of the present study was to evaluate the effects of GA on ccRCC development and clarify the role of autophagy in this process. In the present study, the effects of GA on the proliferation, migration and invasion of ccRCC cells were investigated *in vitro* by Cell Counting Kit-8, colony formation, flow cytometry, wound healing and Transwell migration assays, respectively. Additionally, the effects of GA on ccRCC growth and metastasis were evaluated using hematoxylin-eosin and immunohistochemical staining *in vivo*. Moreover, it was sought to explore the underlying molecular mechanisms using transmission electron microscopy, western blotting and reverse transcription-quantitative PCR analyses. In the present study, it was revealed that GA had a more potent viability inhibitory effect on ccRCC cells (786-O and ACHN) than the effect on normal renal tubular epithelial cell (HK-2), which demonstrated that GA selectively inhibits the viability of cancer cells. Furthermore, it was identified that GA dose-dependently inhibited the proliferation, migration and invasion of ccRCC cells *in vitro* and *in vivo*. It was demonstrated that GA promoted the release of autophagy markers, which played a role in regulating the PI3K/Akt/Atg16L1 signaling pathway. All the aforementioned data provided evidence for the great potential of GA in the treatment of ccRCC.

Correspondence to: Dr Yang Su, Department of Urology, The First Affiliated Hospital of Anhui Medical University, 218 Ji Xi Road, Hefei, Anhui 230032, P.R. China
E-mail: suyang_487@163.com

Key words: gallic acid, autophagy, proliferation, metastasis, clear cell renal cell carcinoma

Introduction

Renal cell carcinoma, originating from the epithelial system of the renal tubules, referred to as kidney cancer, is one of the most prevalent malignant tumors of the urinary system. It constitutes 3% of all adult malignancies and accounts for an estimated 80-85% of renal malignancies (1).

According to the statistics, its incidence ranks the third place in the urinary tumors, and second only to bladder cancer and prostate cancer in China (2). The epidemiological survey revealed that there were 63,000 new cases and 14,000 death cases of RCC in US in 2016, rendering it the 9th most common cancer. Furthermore, its incidence is still increasing every year (3). RCC can be divided into different subtypes in histopathology, the most frequent of which is clear cell RCC (ccRCC), which accounts for 70-80% of all renal malignancies. As RCC lacks early clinical symptoms, nearly 20-30% of patients have metastasized when diagnosed, and the 5-year survival rate of these patients is only 10%, and the median survival is 1 year (4). The radical nephrectomy is the main treatment for localized RCC and has a favorable clinical effect; however, metastatic RCC has lost the indications for surgery, mainly based on the conservative treatments (5). Unfortunately, RCC is not sensitive to traditional radiotherapy and chemotherapy,

and the cytokines are also difficult to achieve the desired therapeutic effect (6). Despite the fact that targeted medicines can significantly prolong progression-free survival and overall survival of patients with metastatic RCC, as well as enhance their quality of life, cytotoxicity and drug tolerance are still existing (7). Therefore, exploring a new effective therapeutic method is becoming a hot topic in the research field of RCC (especially for ccRCC).

In recent years, several studies suggested that plant-derived food (such as polyphenols) intake is associated with increased anticancer benefits for health (8). Gallic acid (3,4,5-trihydroxybenzoic acid, GA) is an endogenous and naturally occurring plant polyphenol which is widely distributed in various plants, fruits and foods worldwide, including tea, oak, chestnut, grapes, strawberries, bananas, red wine, vinegar and others as well as Chinese medicinal herbs (9,10). GA can be absorbed very well by the human organism. It is a yellow-white crystal with melting point at 250˚C and water solubility 1.1% at 20˚C. Its molecular mass is 170.12 g/mol and its chemical formula is $C_6H_2(OH)_3COOH$ (11). GA was initially reported as a free radical scavenger and cell differentiation inducer. It was subsequently reported to exhibit a range of biological and pharmacological properties, including antibacterial, antiviral, antioxidant and anti-inflammatory activities, especially for its antitumor activity (12). Of note, GA was proved to have selective cytotoxicity on certain cancer cells with very less damage to the normal cells (13,14). GA has diverse effects on various tumors at different molecular levels. These features make it a valuable supplement to reduce the risk of tumorigenesis. Polyphenols were reported by numerous studies to exert the anticancer effects via a pleiotropic molecular mechanism of action on cell apoptosis and angiogenesis (15,16). However, with the deepening of the research on the molecular mechanism of cancer development, certain studies previously reported that polyphenols could induce autophagy of cancer cells with dissimilar potencies (17-19). As GA is a well-known polyphenol, it was hypothesized that GA plays a significant role in anticancer activities by regulating autophagy.

To our knowledge, autophagy is a dynamic and evolutionarily conserved process by which cells degrade their long-lived proteins and damaged components (20). Briefly, it is one kind of catabolic pathway and begins with the formation of autophagosomes with double or multi-layer membrane structure. Subsequently, the autophagosomes fuse with the lysosomes to form autolysosomes with single layer membrane structure. Finally, the contents are degraded by the hydrolases in lysosomes and recycled. As a result, cells digest and recycle nutrients or damaged organelles via autophagy, which improves cell survival in conditions of inadequate nutrition or oxygen availability (21). However, excessive autophagy may also result in autophagic cell death (22). There is growing evidence that autophagy plays a crucial role in the regulation of tumorigenesis. Among them, certain studies indicated that autophagy functions as tumor suppressor, while the others argued that autophagy could promote tumor survival and progression (23). The issue, whether autophagy represents a mechanism that allows tumor cells to survive from therapy or a mechanism that initiates a non-apoptotic cell death type is being debated. Additionally, there are limited studies with regard to the effects of GA on RCC cells. Therefore, in order to further address GA and its potential autophagy regulating character, the roles of GA in RCC development were investigated in the present study.

Materials and methods

Reagents. GA with 99% purity and 3-methyladenine (3-MA) were obtained from MilliporeSigma. Roswell Park Memorial Institute-1640 medium (RPMI-1640), fetal bovine serum (FBS), penicillin-streptomycin were purchased from Gibco; Thermo Fisher Scientific, Inc. Cell Counting Kit-8 (CCK-8) was acquired from Dojindo Laboratories, Inc. PI/RNase Staining Buffer kit and Matrigel were obtained from BD Biosciences. The primary antibodies against PI3K, phosphorylated (P-)PI3K, Akt, P-Akt, Atg16L1 and P-Atg16L1 were purchased from Cell Signaling Technology, Inc. The primary antibodies against LC3B, Beclin-1, P62 and GAPDH were purchased from Abcam. The secondary antibody was obtained from LI-COR Biosciences. PrimeScipt™ RT reagent Kit with gDNA Eraser and SYBR@Premix Ex Taq™ II were obtained from Takara Bio, Inc.

Cell culture and drug preparation. The ccRCC cell lines (786-O and ACHN) and the normal renal tubular epithelial cell (HK-2) were obtained from Cell Bank of Wuhan University (Wuhan, China). The cells were cultured in RPMI-1640 medium (Gibco; Thermo fisher scientific, Inc.) with 10% FBS, 100 units/ml penicillin and 100 units/ml streptomycin, then maintained in 37˚C with 5% CO_2 incubator (Binder GmbH). The GA and 3-MA stock solution was respectively prepared at a concentration of 73,477 μmol/l and 166 mmol/l: respectively added 0.5 g GA and 2.5 g 3-MA into a EP tube, respectively added 40 and 100 ml FBS-free RPMI-1640 medium, respectively mixed on a vortex oscillator to ensure the complete dissolution, and then stored at -20˚C. Before application, the GA and 3-MA stock solution should be appropriately diluted and heated. To generate the working solution (GA: 0, 5, 10 and 20 μmol/l; 3-MA: 5 mmol/l), the GA and 3-MA stock solutions were taken out, dissolved at 37˚C, and then diluted to the designated concentration with FBS-free RPMI-1640 medium. In addition, the light should be avoided in the period of GA and 3-MA using.

Cell viability assay. The ccRCC cells (786-O and ACHN) and the normal renal tubular epithelial cell (HK-2) were first plated in a 96-well plate at $5x10^3$ cells/well for 24 h of incubation at 37˚C for the CCK-8 assay. The preceding medium was then taken out, and 100 μl of 0, 5, 10, 20 μmol/l GA solution was placed into each well for 24, 48 and 72 h of stimulation, respectively. When the scheduled time arrived, the preceding medium was replaced with 100 μl new RPMI-1640 medium containing 5% CCK-8. A microplate reader (PerkinElmer, Inc.) was used to measure the absorbance at 450 nm following 1 h of incubation at 37˚C in the dark. The half maximal inhibitory concentration (IC_{50}) and inhibition rate were then calculated for each group.

Plate clone formation assay. The ccRCC cells (786-O and ACHN) were initially plated into the six-well plate and cultured for 48 h. The cells were treated with varying concentrations

of GA (0, 5, 10 and 20 μmol/l) for a duration of 24 h. Upon completion, the cells in each well were digested, counted, and plated into a new six-well plate at a seeding density of $1x10^3$ cells/well with complete medium. They were then cultured consecutively for one week at 37˚C. Subsequent to removal of the medium, the cells were washed with phosphate buffered saline (PBS) for 3 times. Following this, the cells were fixed using a 4% paraformaldehyde solution for 20 min at room temperature (RT), and subsequently stained with a 0.5% crystal violet solution for 20 min at RT. The stained cells were ultimately washed with PBS and air-dried, and the number of colonies was counted manually. The minimum number of cells required for colony formation was 50-100.

Cell cycle analysis. The ccRCC cells (786-O and ACHN) were firstly stimulated with different concentrations of GA solution (0, 5, 10 and 20 μmol/l) for 24 h. The cells were then collected and washed with PBS. Each tube received 1 ml 70% ethanol and was incubated at -20˚C overnight for fixing. Following that, the fixed ccRCC cells were collected and washed with 4˚C PBS, and 500 μl PI/RNase dye solution was added into each tube and incubated for 10 min at 25˚C in the dark. Finally, flow cytometry (FACSCanto II cytometer; BD Biosciences) was used to measure the fluorescence intensity of each group in real time and analyzed by FlowJo software (Tree Star, Inc.).

Wound healing assay. The ccRCC cells (786-O and ACHN) from each group were plated in six-well plates for 48 h. After the cell density reached ~80%, the monolayer was wounded by scratching it lengthwise along the plate surface with a 200-μl sterile pipette tip. The medium was then removed, and the cells were washed twice with PBS and cultured in serum-free RPMI-1640 medium. To capture images of cell migration, an inverted microscope was used (Olympus Corporation) and recorded at 0, 12 and 24 h. Finally, the area of migration (μm^2) was measured using the ImageJ software (Version 1.53; National Institutes of health).

Transwell migration and Matrigel invasion assays. The Transwell migration and invasion assays were performed on ccRCC cells (786-O and ACHN) stimulated with varying concentrations of GA solution (0, 5, 10 and 20 μmol/l). After 24 h of stimulation, the cells were collected by trypsin and suspended in FBS-free RPMI-1640 medium. The cell density was adjusted and 100 μl of $2x10^5$ cells/ml ccRCC cell suspension was added to the upper Boyden chamber (8-μM pore size; Corning, Inc.). The lower chamber was filled with 700 μl RPMI-1640 medium containing 20% FBS. The 24-well plate was then placed in a 37˚C incubator. After 24 h of incubation, the Transwell chamber was removed from the incubator and non-migratory cells were scraped with a cotton swab. The migratory cells were fixed with 4% paraformaldehyde for 20 min at RT and dyed with 0.5% crystal violet solution for another 20 min. The migratory cells were observed and images were captured using an inverted light microscope (Olympus Corporation). The cells in 5 randomly selected fields were counted and the mean was calculated. Matrigel was diluted 1:8 with FBS-free RPMI-1640 media on ice for the Matrigel invasion assay. The upper chambers of the Transwell were coated with 80 μl of the diluted Matrigel. The next processes were identical to the migration experiments.

Western blot analysis. The proteins of ccRCC cells were extracted using RIPA lysis buffer (Thermo Fisher Scientific, Inc.) and phosphatase inhibitors were added to prevent sample degradation. Protein concentrations were measured with a bicinchoninic acid protein assay kit (Beyotime Institute of Biotechnology), and electrophoresed on sodium dodecyl sulfate-polyacrylamide gels with varying concentrations of 8, 12, or 15%. The proteins were then transferred onto polyvinylidene difluoride membranes (MilliporeSigma). After blocking for 1 h at RT with 5% skimmed milk in Tris-buffered saline containing 0.1% Tween-20 (TBST) and washing three times with TBST, the membranes were incubated overnight at 4˚C with the specified monoclonal primary antibodies (1:1,000-2,000). The membranes were then washed 3 times with TBST and incubated with the corresponding goat-anti-rabbit secondary antibody (1:20,000) at RT for 1 h. After washing 3 times with TBST, the membranes were scanned with a two-color infrared imaging system (LI-COR, Biosciences). GAPDH was used as an internal reference. Densitometric analysis was performed using ImageJ software.

Reverse transcription-quantitative PCR (RT-qPCR). Total RNA was isolated from ccRCC cells (786-O and ACHN) using TRIzol reagent (Invitrogen; Thermo fisher scientific, Inc.). AB7500 detection system (Thermo fisher scientific, Inc.) was used to measure the reverse transcription reactions, which were carried out using a PrimeScriptTM RT reagent kit (Takara Bio, Inc.) in accordance with the manufacturer's instructions. qPCR reactions were prepared using a SYBR Green Mix (Takara Bio, Inc.) at a final volume of 20 μl. The relative gene expression level was calculated using the $2^{-\Delta\Delta Cq}$ method. The data were normalized using an internal control called GAPDH. Three duplicates of each response were carried out. Primer sequences are displayed in Table I.

Transmission electron microscopy (TEM). The ccRCC cells (786-O and ACHN) were collected and fixed with 2.5% glutaraldehyde at 4˚C for 2 h and 1% osmium tetroxide for 30 min and then dehydrated in a graded series of ethanol. The cells were embedded in epoxy resin and sectioned at 70-nm thickness using an ultramicrotome. The sections were stained with 0.2% lead citrate and 2% uranyl acetate. The images were captured with a transmission electron microscope (Hitachi, Ltd.).

Xenografts and tumor metastasis model. Female BALB/c nude 4-week-old mice (n=48) weighing 20±2 g were acquired from the Wuhan University Animal Experiment Center (Wuhan, China). All animals were housed in a specific pathogen-free environment (12/12-h light/dark cycle; *ad libitum* access to food and water) with the right humidity and temperature. Each mouse received an injection of 200 μl of PBS containing ~$1x10^7$ 786-O cells and ACHN cells in the left flank. Every week after inoculation, tumor volume was measured and computed using the formula (length x $width^2$)/2. The nude mice were separated into 4 groups of 3 mice each after the average tumor volume reached ~100 mm^3 (~10 days later). The mice received freshly prepared solutions (the only source

Table I. List of primers used for reverse transcription-quantitative PCR.

Gene name	Primer sequence (5'→3')
LC3B	F: GGCTTTCAGAGAGACCCTGAG
	R: CCGTTTACCCTGCGTTTGTG
Beclin-1	F: CCACAGAAAGTGCCAACAGC
	R: GACGTTGAGCTGAGTGTCC
P62	F: GGTCGCGCTCACCTTTCT
	R: GGAGATGAGGCTCCGCAAT
GAPDH	F: AAAGCCTGCCGGTGACTAAC
	R: TTCCCGTTCTCAGCCTTGAC

F, forward; R, reverse.

of drinking water) every Monday, Wednesday, and Friday after the weighted GA powder was separately dissolved in the water to form solutions with varying concentrations of GA (w/v) (0.3, 0.6 and 0.9% in regular drinking water). The control mice were given access to regular water during this time. All mice were administered an excessive dose of carbon dioxide for euthanasia after two months, and the weight of the tumors was measured immediately. Additionally, the tumor metastasis model was created by injecting 786-O and ACHN cells into the tail veins of additional BALB/c nude mice. To do this, $1x10^6$ cells mixed with PBS were injected into each mouse in 4 groups (n=3 per group), and the mice were then administered drinks containing various concentrations of GA solution. After 2 months, all mice were euthanized with an overdose of carbon dioxide, and the weight of tumors was measured immediately. Displacement rate of CO_2 used for euthanasia was 30%. All animal studies were approved by the Animal Care and Use Committee of Anhui Medical University (approval no. LLSC20232011; Hefei, China), and all animal experiments were carried out in accordance with the National Institutes of Health's Guide for the Care and Use of Laboratory Animals.

Hematoxylin-eosin (H&E) staining. The lung tissues were fixed in 4% paraformaldehyde to cause coagulation and denaturing of proteins at RT for 8 h. All samples were dehydrated in an ethanol gradient and xylene. Subsequently, the tissues were embedded in paraffin, cooled and solidified into blocks. Afterwards, paraffin blocks were cut into 4-μm-thick slices. The sections were then stained with hematoxylin and eosin and images were captured by light microscopy (Olympus Corporation).

Immunohistochemistry (IHC) assay. For antigen retrieval, the paraffin-embedded tumor sections were heated at 105˚C for 10 min in a citric acid buffer (0.01 M) and then deparaffinized in xylene for 15 min. Following a 10-min PBS washing, the slides were put into a 5-min immersion in a 3% hydrogen peroxide solution to inhibit endogenous peroxidase activity. The sections were then washed once more in PBS for 5 min, blocked with the blocking solution for 1 h at RT, and then incubated with the appropriate antibody for 1 h at RT. Finally, an immunochemistry kit (OriGene Technologies, Inc.) was used to find the immune complexes. A light microscope (Olympus Corporation) was used to observe the sections.

Statistical analysis. At least three independent times of each experiment were conducted. The mean ± standard deviation (SD) was used to represent the data. The treatment groups were compared using one-way analysis of variance (ANOVA) with SPSS 22.0 (SPSS, Inc.). Bonferroni's post hoc test was used. $^*P<0.05$ was considered to indicate a statistically significant difference.

Results

GA inhibits the viability of ccRCC cells. In a previous study by the authors, the effects of each monomer in pomegranate peel tannins on human bladder cancer T24 cells viability were compared, and it was found the inhibition of GA on T24 cells viability was significantly higher than the other three monomers, which indicated that GA is the effective anticancer component in pomegranate peel tannins (24). Therefore, in order to measure the effects of GA on ccRCC cells (786-O and ACHN) and renal tubular epithelial cell (HK-2) viability, CCK-8 assay was used. The findings revealed that, when compared with the control group, the vitality of the 786-O and ACHN cells in the GA-treated group was considerably reduced ($P<0.05$), whereas that of the HK-2 cells was not significantly affected. These findings demonstrated that GA significantly decreased the viability of 786-O and ACHN cells in a time- and concentration-dependent manner, but not HK-2 cells. As demonstrated in Fig. 1A-C, the IC_{50} of GA stimulating 786-O cells for 24, 48 and 72 h were 4.20, 2.89 and 2.39 μmol/l respectively, while the IC_{50} of GA stimulating ACHN cells for 24, 48 and 72 h were 10.51, 7.05 and 2.75 μmol/l, respectively. These findings revealed that GA significantly reduced the viability of 786-O and ACHN cells, especially when stimulated for 24 h ($P<0.05$). As a consequence, GA with 0, 5, 10 and 20 μmol/l was identified as the suitable action concentration and 24 h as the optimum action period, combining with the results of CCK-8.

GA changes the morphology of ccRCC cells. To study the effect of GA on ccRCC cell morphology, an inverted microscope was utilized and it was observed that both the 786-O and ACHN cells exhibited elongation, robust adhesion, large cellular frames, clear cell outlines, and overall exhibited signs of favorable condition. Following 24-h GA stimulation, the 786-O and ACHN cells demonstrated a notable decrease in size, weakened adhesive properties, reduced intercellular connections, blurred cellular outlines, and appeared to be in a state of cellular death (Fig. S1A and B).

GA inhibits proliferation of ccRCC cells. To further evaluate the effect of GA on ccRCC cell proliferation, a plate clone formation assay was utilized. The results from the plate cloning assay indicated a significant decrease in the number of colonies for both 786-O and ACHN cells in the GA-treated groups, compared with the control group. Notably, the number of colonies decreased consistently with increasing concentrations of GA (Fig. 1D-G). The results indicated that

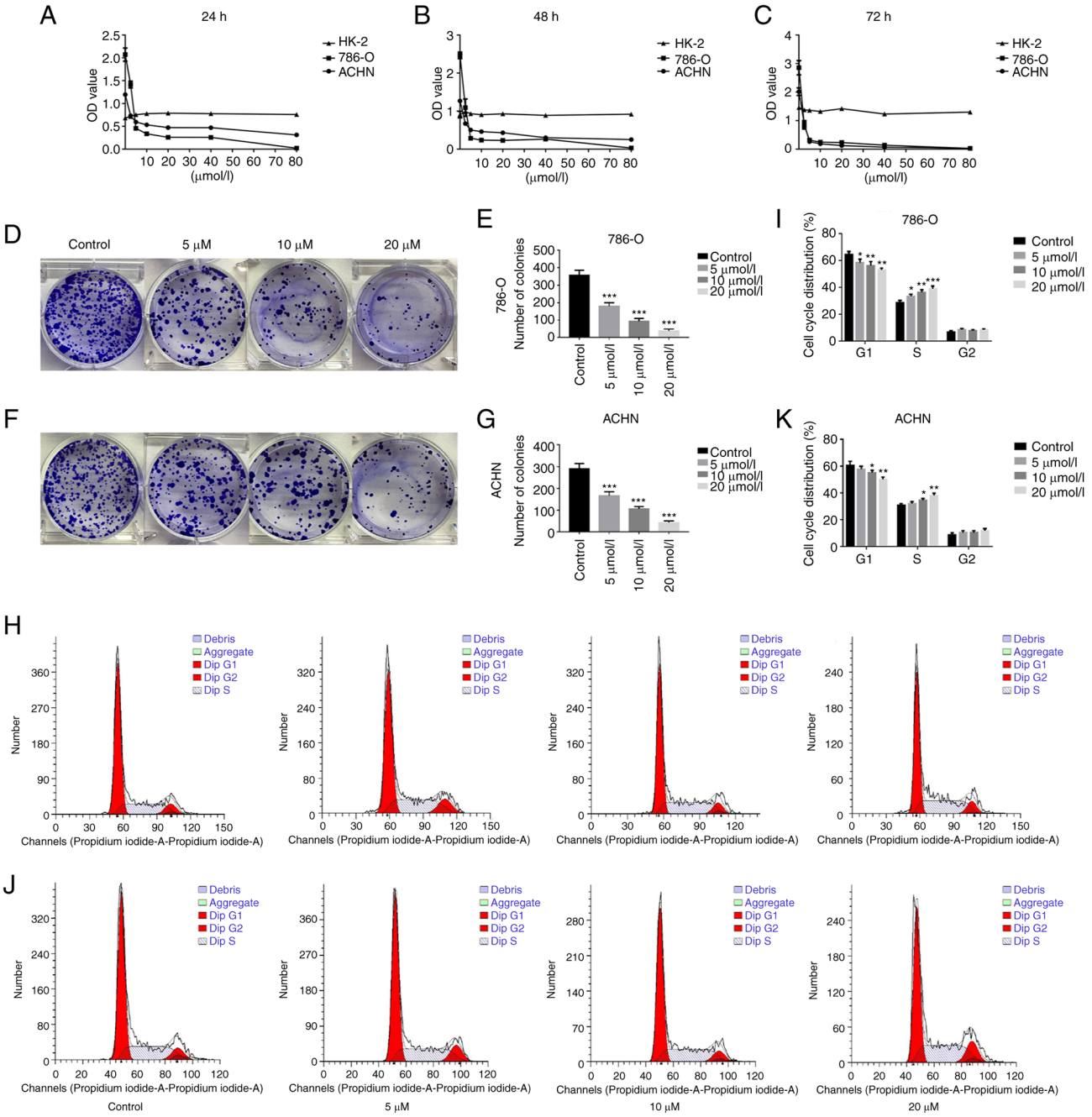

Figure 1. GA inhibits viability and proliferation of ccRCC cells as well as affects cell cycle distribution. (A-C) The viability of ccRCC cells and normal renal tubular epithelial cell with different concentrations of GA treatment in 24, 48 and 72 h were measured by Cell Counting Kit-8 assay. (D-G) Representative images and quantitative analyses of ccRCC cells' colonies in each group were displayed according to the plate cloning assays. (H-K) Representative images and quantitative analyses of ccRCC cells cycle status were assessed by flow cytometry. *P<0.05, **P<0.01 and ***P<0.001 compared with the control group. GA, gallic acid; ccRCC, clear cell renal cell carcinoma.

GA significantly suppressed proliferation of ccRCC cells in a concentration-dependent way.

GA blocks the cycle process of ccRCC cells. To evaluate the effect of GA on the cell cycle of ccRCC cells, flow cytometry was employed. The results demonstrated that the control group had 63.19% 786-O cells in G1 phase and 28.71% in S phase (Fig. 1H and I). Additionally, the results for the control group revealed that 60.53% of ACHN cells were in G1 phase, while 31.72% were in S phase (Fig. 1J and K). In addition, as the concentration of GA increased, there was a significant increase in the number of 786-O and ACHN cells in S phase, accompanied by a significant decrease in the number of cells in G1 phase (P<0.05). In summary, the findings indicated that GA effectively hindered the cell cycle of ccRCC cells specifically in the S phase.

GA inhibits migration and invasion of ccRCC cells. The wound healing and the Transwell assays were used to evaluate the effects of GA on the migration and invasion of ccRCC cells. It was identified that, in comparison with the control group, the GA-treated group significantly inhibited the

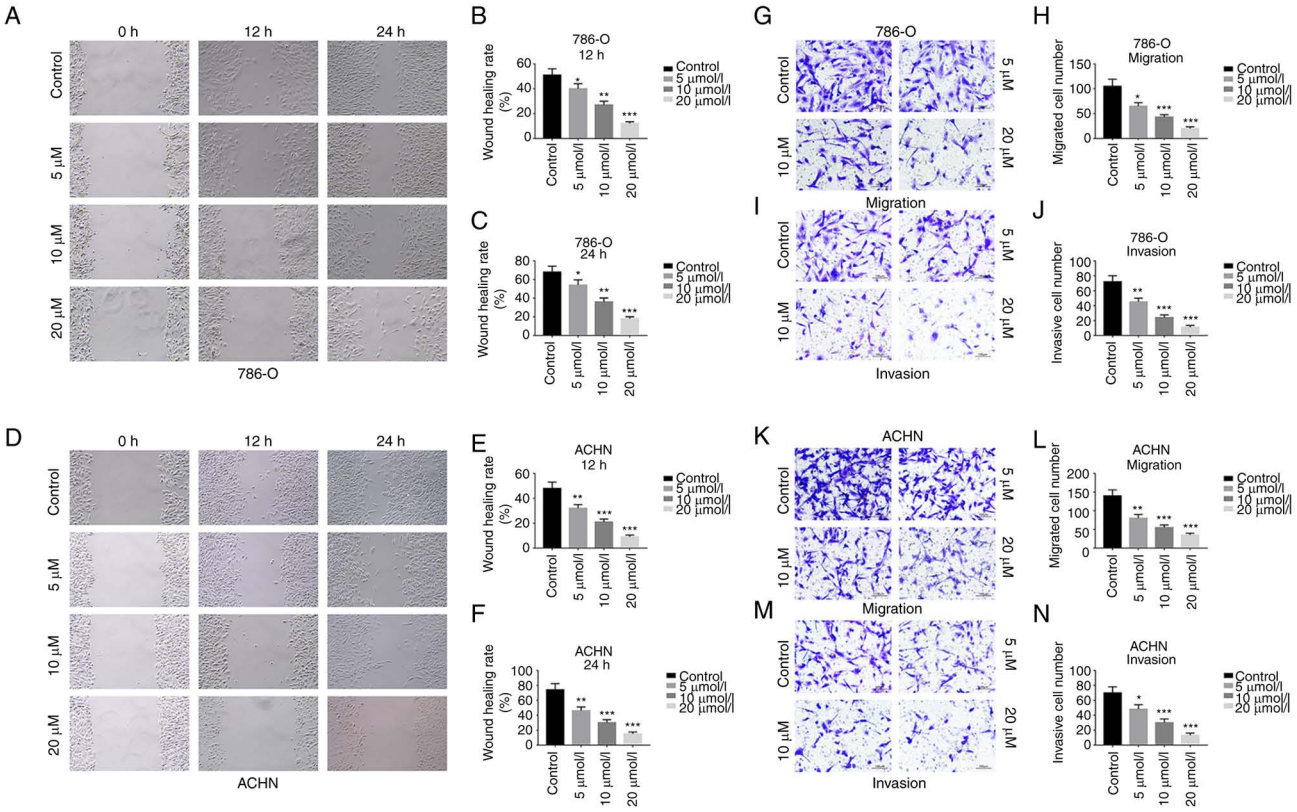

Figure 2. Gallic acid inhibits migration and invasion of ccRCC cells *in vitro*. (A-F) Representative images and quantitative analyses of ccRCC cells' migration rates in each group were shown according to the wound healing assay (magnification, x100). (G, H, K and L) Representative images and quantitative analyses of migratory (G and H) 786-O cells and (K and L) ACHN cells in each group were demonstrated according to Transwell migration assay (magnification, x200). (I, J, M and N) Representative images and quantitative analyses of invasive (I and J) 786-O cells and (M and N) ACHN cells in each group were displayed according to Matrigel invasion assay (magnification, x200). *P<0.05, **P<0.01 and ***P<0.001 compared with the control group. ccRCC, clear cell renal cell carcinoma.

migration of 786-O and ACHN cells, and that the inhibition rate was dependent on the concentration of GA (Fig. 2A-F). Moreover, the Transwell migration assay demonstrated that GA treatment led to a significant decrease in the number of 786-O cells (Fig. 2G and H) and ACHN cells (Fig. 2K and L) that had passed through the chamber membrane. Furthermore, it was observed that the number of 786-O (Fig. 2I and J) and ACHN (Fig. 2M and N) cells that passed through the Matrigel and chamber membrane decreased as the concentration of GA increased in the Matrigel invasion assay. These results indicated that GA significantly inhibited migration and invasion of ccRCC cells in a concentration-dependent way.

GA inhibits growth and metastasis of ccRCC. To investigate the effect of GA on the growth and metastasis of ccRCC, xenograft and tumor metastasis models were established. In both models, 786-O and ACHN cells were used, and it was found that tumors were successfully formed in all mice injected with these cells (Fig. 3A-C and G-I, respectively). Moreover, the weight and volume of tumors were significantly lighter and smaller in the GA-treated group than in the control group. The IHC results revealed a significant decrease in the expression of Ki-67 (a marker of proliferation) and MMP-9 (a marker of metastasis) in the GA-treated group compared with the control group for both 786-O cells (Fig. 3D and E) and ACHN cells (Fig. 3J and K). Finally, the H&E staining results demonstrated that compared with that in the control group, 786-O cells (Fig. 3F) and ACHN cells (Fig. 3L) metastasized into the lungs were significantly decreased in the GA-treated group. The quantification of representative IHC and H&E images is demonstrated in Fig. S2. These results indicated that ccRCC growth and metastasis were significantly inhibited by GA in a concentration-dependent way.

GA induces autophagy in ccRCC. To investigate the correlation between GA and autophagy in ccRCC, the expression of autophagy-related markers was examined. Firstly, the western blotting results revealed that compared with that in the control group, LC3B-II and Beclin-1 protein expression was significantly increased, while P62 protein expression was significantly decreased in the GA-treated groups (Fig. 4A-H). Meanwhile, RT-qPCR results demonstrated significantly increased LC3B and Beclin-1 gene transcription and significantly decreased P62 gene transcription in the GA-treated groups than in the control group (Fig. 4I-N). Subsequently, the TEM revealed a significantly higher number of autophagosomes in the groups treated with GA compared with the control group (Fig. 5A-D). Moreover, the IHC results indicated that LC3B expression was significantly increased in the tumors of GA-treated groups than in the tumors of control group (Fig. 4O and P). In addition, the western blotting results revealed that LC3B-II and Beclin-1 protein expression

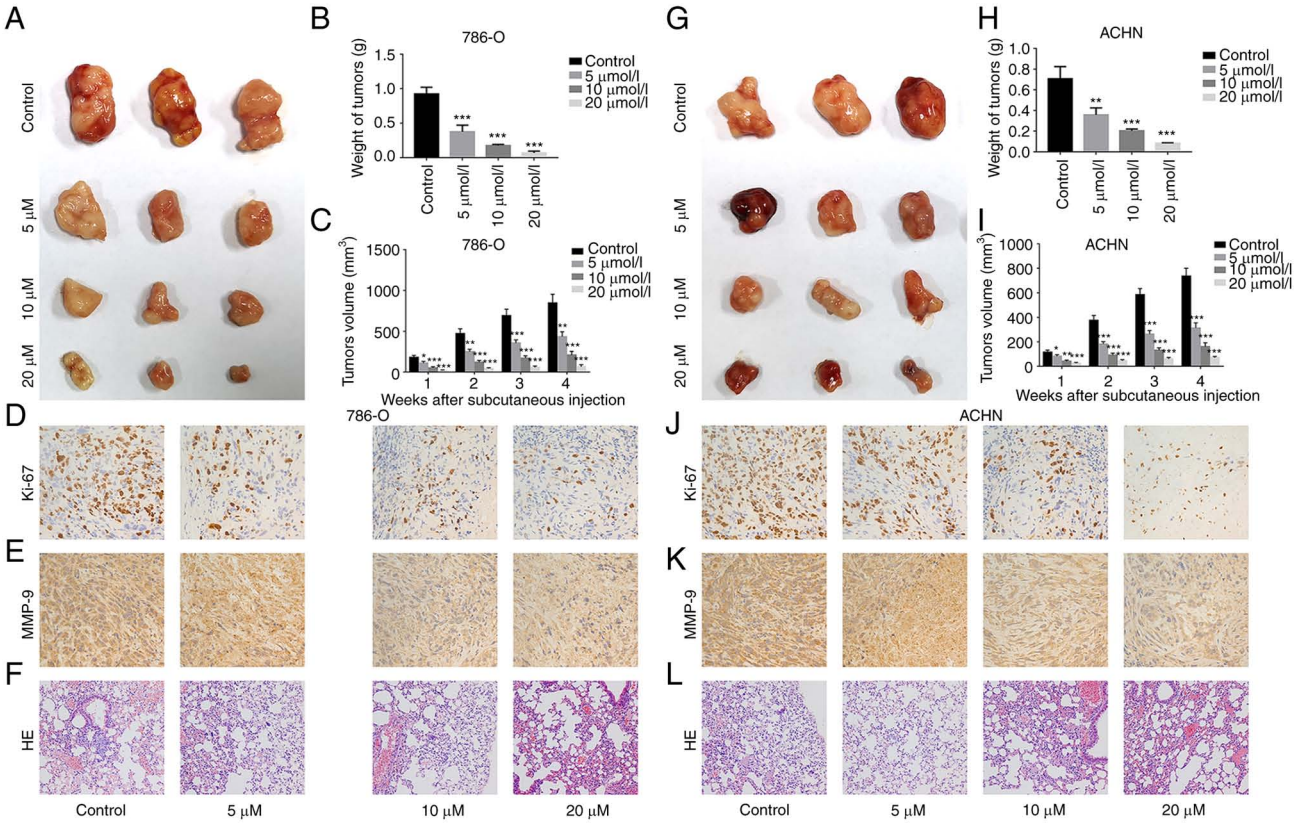

Figure 3. GA inhibits clear cell renal cell carcinoma growth and metastasis *in vivo*. (A-C and G-I) Representative images of the (A and G) isolated tumors as well as the (B and H) weight and (C and I) volume analyses of the tumors from 786-O cells and ACHN cells in different concentrations of GA-treated groups. (D-L) Representative immunohistochemistry images of (D and J) Ki-67 and (E and K) MMP-9 expression in the tumors from 786-O cells and ACHN cells in different groups are displayed (magnification, x400). (F and L) Representative H&E staining images of (F) 786-O cells and (L) ACHN cells metastasized into the lungs of mice from different groups (magnification, x200). *P<0.05, **P<0.01 and ***P<0.001 compared with the control group.

was significantly decreased and P62 protein expression was significantly increased in the GA (IC_{50}) + 3-MA treatment group compared with the GA (IC_{50}) group (Fig. 6A-H). These results indicated that GA could induce ccRCC autophagy *in vivo* and *in vitro*.

GA inhibits proliferation of ccRCC cells by inducing autophagy. In order to assess the role of autophagy in the inhibition of GA on ccRCC cells proliferation, 3-MA (a common autophagy inhibitor) was added on the basis of GA (IC_{50}) stimulation. The CCK-8 results demonstrated that viability of 786-O and ACHN cells was significantly inhibited in the GA (IC_{50}) group compared with the control group, while the inhibitory effects of GA (IC_{50}) on 786-O and ACHN cells were significantly reversed by 3-MA (Fig. 7A-F). The plate clone formation assay indicated that there were fewer colonies of 786-O and ACHN cells in the GA (IC_{50}) group compared with the control group, while the reduction trend on the colonies of 786-O and ACHN cells were significantly reversed by 3-MA (Fig. 7G-J). These results indicated that GA could suppress proliferation of ccRCC cells by inducing autophagy.

GA inhibits migration and invasion of ccRCC cells by inducing autophagy. In order to further assess the role of autophagy in the inhibition of GA on ccRCC cells migration and invasion, 3-MA was added on the basis of GA (IC_{50}) stimulation. According to the results of the Transwell migration assay, treatment with GA (IC_{50}) led to a significant reduction in the number of migratory 786-O and ACHN cells compared with the control group. On the other hand, the migration of 786-O and ACHN cells was significantly increased after treatment with 3-MA, reversing the effect observed with GA (Fig. 7K-N). Moreover, the Matrigel invasion assay results indicated that there were fewer invasive 786-O and ACHN cells number in the GA (IC_{50}) group than in the control group, while the invasion results of 786-O and ACHN cells were significantly reversed by 3-MA (Fig. 7O-R). These results indicated that GA could suppress migration and invasion of ccRCC cells by inducing autophagy.

GA induces autophagy of ccRCC cells via the PI3K/Akt/Atg16L1 signaling pathway. In order to explore the mechanism involved in the induction of ccRCC cells autophagy by GA, the transcription of related genes and the expression of critical protein were assessed in ccRCC cells (786-O and ACHN). Firstly, the RT-qPCR results revealed that Atg16L1 gene expression was significantly increased in both 786-O and ACHN cells (Fig. 8A and B). Subsequently, the western blotting results demonstrated that compared with that in the control group, P-PI3K and P-Akt protein expression levels were significantly decreased, while Atg16L1 protein expression was significantly increased in the GA-treated groups (Fig. 9A-N). These results indicated that GA could induce autophagy in ccRCC cells via the PI3K/Akt/Atg16L1 signaling pathway.

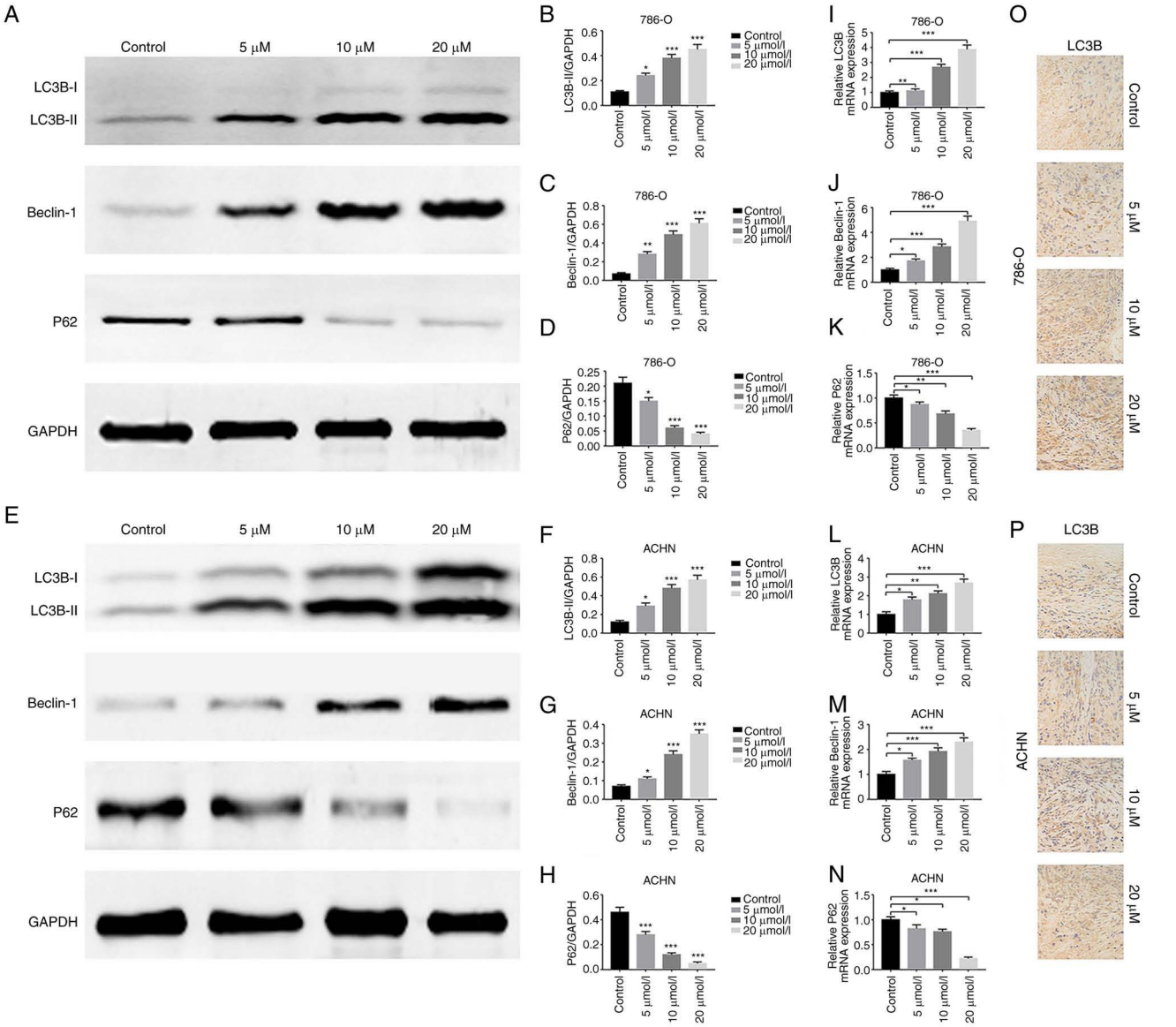

Figure 4. GA induces autophagy of ccRCC cells. (A-H) Representative western blotting images and quantitative analyses of autophagy markers, including (B and F) LC3B, (C and G) Beclin-1 and (D and H) P62 in ccRCC cells with different concentrations of GA treatment. (I-N) Reverse transcription-quantitative PCR analyses of autophagy markers, including (I and L) LC3B, (J and M) Beclin-1 and (K and N) P62 in ccRCC cells with different concentrations of GA treatment. (O and P) Representative immunohistochemistry images of LC3B expression in the tumors from ccRCC cells in different groups (magnification, x400). GAPDH was served as the internal reference. *P<0.05, **P<0.01 and ***P<0.001 compared with the control group. GA, gallic acid; ccRCC, clear cell renal cell carcinoma.

Discussion

RCC is a leading cause of cancer-related death as previously reported, especially for ccRCC (25). Therefore, it is particularly important to find an effective and anti-resistance treatment with minor side effects for it. Modern drug research mainly focuses on the identification of effective and safe drugs. Although there are numerous cancer projects at present, the choices in replacing the traditional treatments for cancer patients are very limited. It is estimated that ~49% of drugs that are involved in the treatment of cancers derive from either natural products or their derivatives (26). GA, as a predominant polyphenol, its various biological activities have been reported; however, the major interest in GA is its antitumoral activity. GA has been demonstrated to inhibit the development of several cancer types including leukemia, prostate, lung, oral, pancreatic, glioma, gastric, colon, breast, cervical and esophageal cancer via animal models *in vivo* or via cell lines *in vitro* (27-32). Specifically, the inhibitory effects of GA on cancer progression involve in cell cycle, growth, metastasis, angiogenesis and apoptosis. For example, Lee *et al* (33) reported that GA caused an increase in G0/G1 and sub-G1 phase ratio in breast cancer cells, and found that GA downregulated cyclin D1/CDK4 and cyclin E/CDK2, and upregulated p21 and p27. Lima *et al* (34) presented that GA decreased proliferation of hepatocellular carcinoma cells in a dose-dependent manner without causing necrosis; moreover, GA did not cause regrowth of cancer cells in a long period. Ho *et al* (35) supported that GA inhibited metastasis and invasive growth of gastric cancer cells via RhoB increase, AKT/small GTPase signaling downregulation and NF-κB activity inhibition. Zhao and Hu (9) indicated that GA significantly reduced proliferation of human cervical

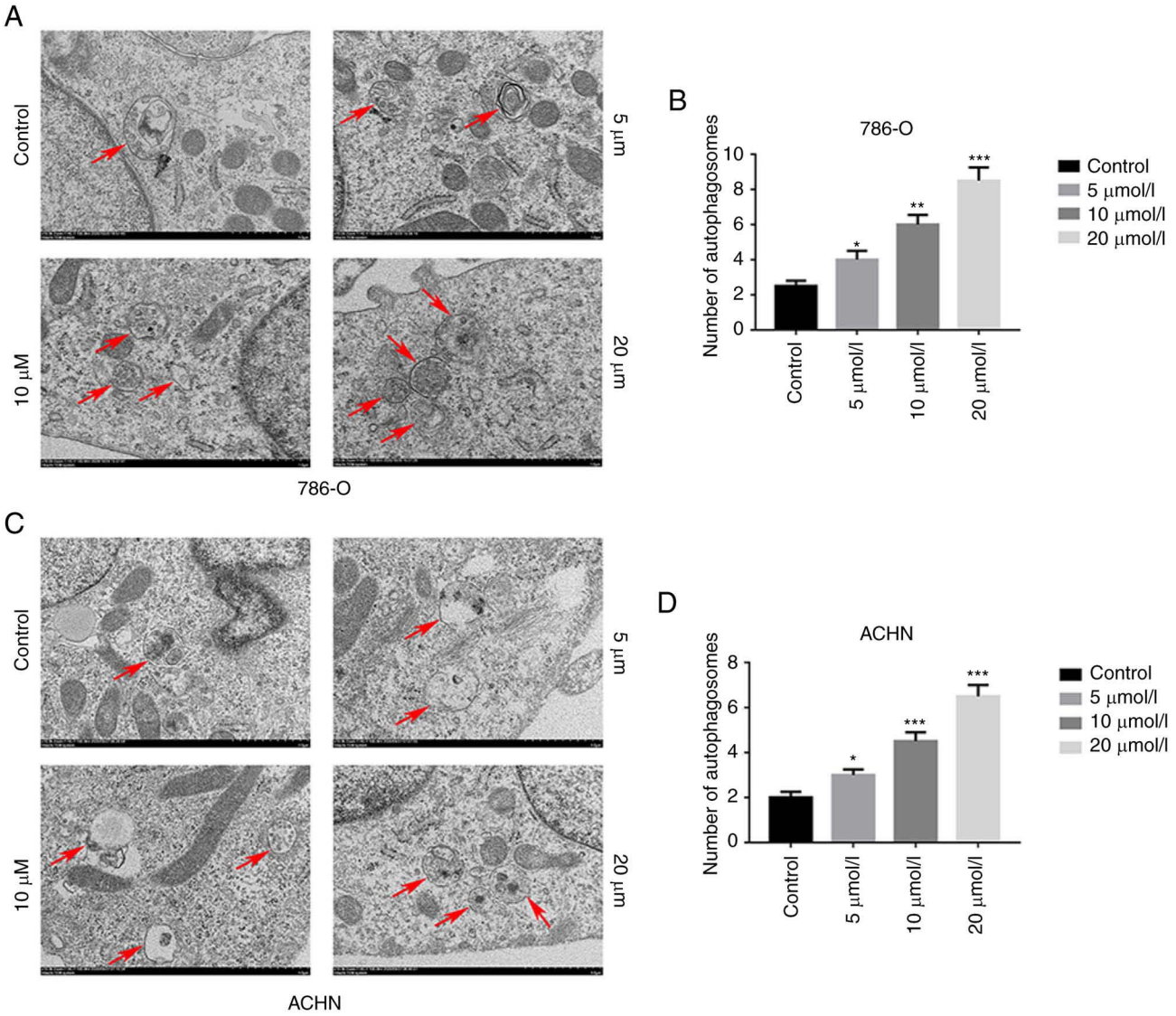

Figure 5. GA induces the formation of autophagosomes in ccRCC cells. (A-D) Red arrows indicate the formation of autophagosomes. Representative transmission electron microscopy images and quantitative analyses of autophagosomes formed in ccRCC cells with different concentrations of GA treatment. *P<0.05, **P<0.01 and ***P<0.001 compared with the control group. GA, gallic acid; ccRCC, clear cell renal cell carcinoma.

cancer cells and the tube formation in human umbilical vein endothelial cells. Subramanian *et al* (36) displayed that GA induced the apoptosis of colon cancer cells with the morphological changes. These actions of GA against cancers make it an important biological molecule for therapeutic use.

Based on the aforementioned discussion, it is concluded that the inhibition of cell proliferation and induction of cell death are the crucial focus for cancers therapy. Chemical drug therapy typically involves the induction of caspase-mediated apoptosis, which is a well-established fact. However, a major obstacle associated with this approach is the development of resistance by cancer cells to drug-induced apoptosis over time (18). Therefore, agents that can induce alternative type of programmed cell death (PCD) may help in breaking this apoptosis-resistance of cancer cells to improve the therapeutic efficiency. Autophagy is a type of PCD, and the existence of this alternative cell death may make the aforementioned inference to be the truth. Autophagy is a cellular process that is conserved throughout evolution. It involves the degradation and recycling of cellular components. The molecular machinery of autophagy has been clarified in yeast and mammals. There are 11 autophagy-related genes (Atgs) and 8 orthologs in mammals, which play a critical role in the autophagy pathway. Atg3, Atg4 and Atg8/LC3 are involved in phagophore expansion, while Atg5 is crucial for generating the Atg12-Atg5 conjugate required for this process. Atg6/Beclin-1 and Atg14 are components of PI3K complexes, which are involved in the induction of autophagy, while Atg7 and Atg10 are E1-like and E2-like enzymes, respectively, that mediate conjugation systems involved in phagophore expansion. Atg9 is a transmembrane protein involved in autophagy induction and Atg13 serves as a binding partner and regulator of Atg1/ULK. Lastly, Atg12 and Atg16L1 are involved in directing LC3 lipidation on autophagosomal membranes, which is essential for phagophore expansion (37).

Recently, the relationship between autophagy and cancers has been extensively studied, indicating that autophagy can

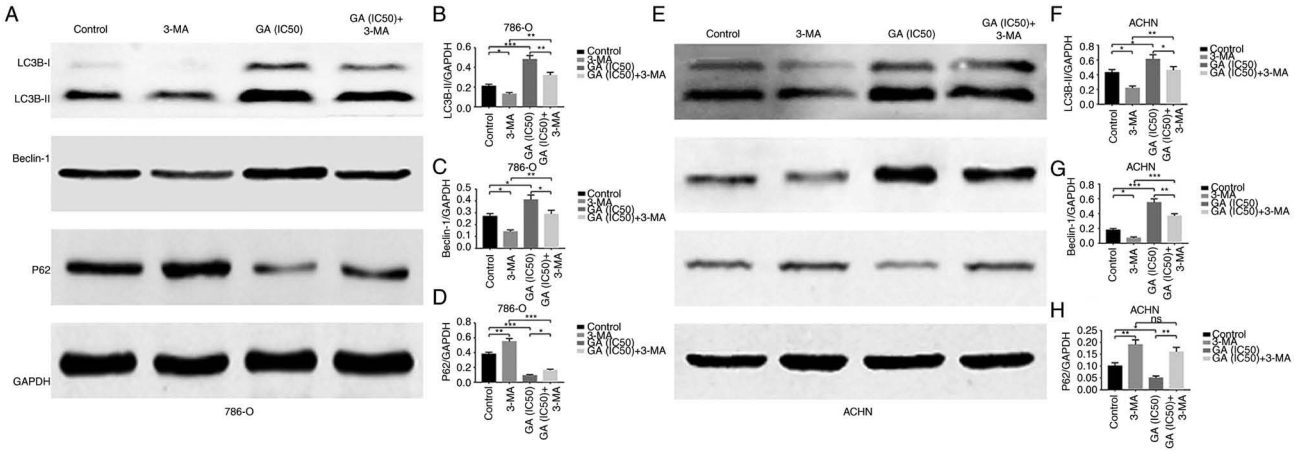

Figure 6. 3-MA reverses autophagy of ccRCC cells induced by GA. (A-H) Representative western blotting images and quantitative analyses of autophagy markers, including (B and F) LC3B, (C and G) Beclin-1 and (D and H) P62 in ccRCC cells in different groups. GAPDH served as the internal reference. *P<0.05, **P<0.01 and ***P<0.001 compared with the control group and GA (IC_{50}) group. 3-MA, 3-methyladenine; ccRCC, clear cell renal cell carcinoma; GA, gallic acid.

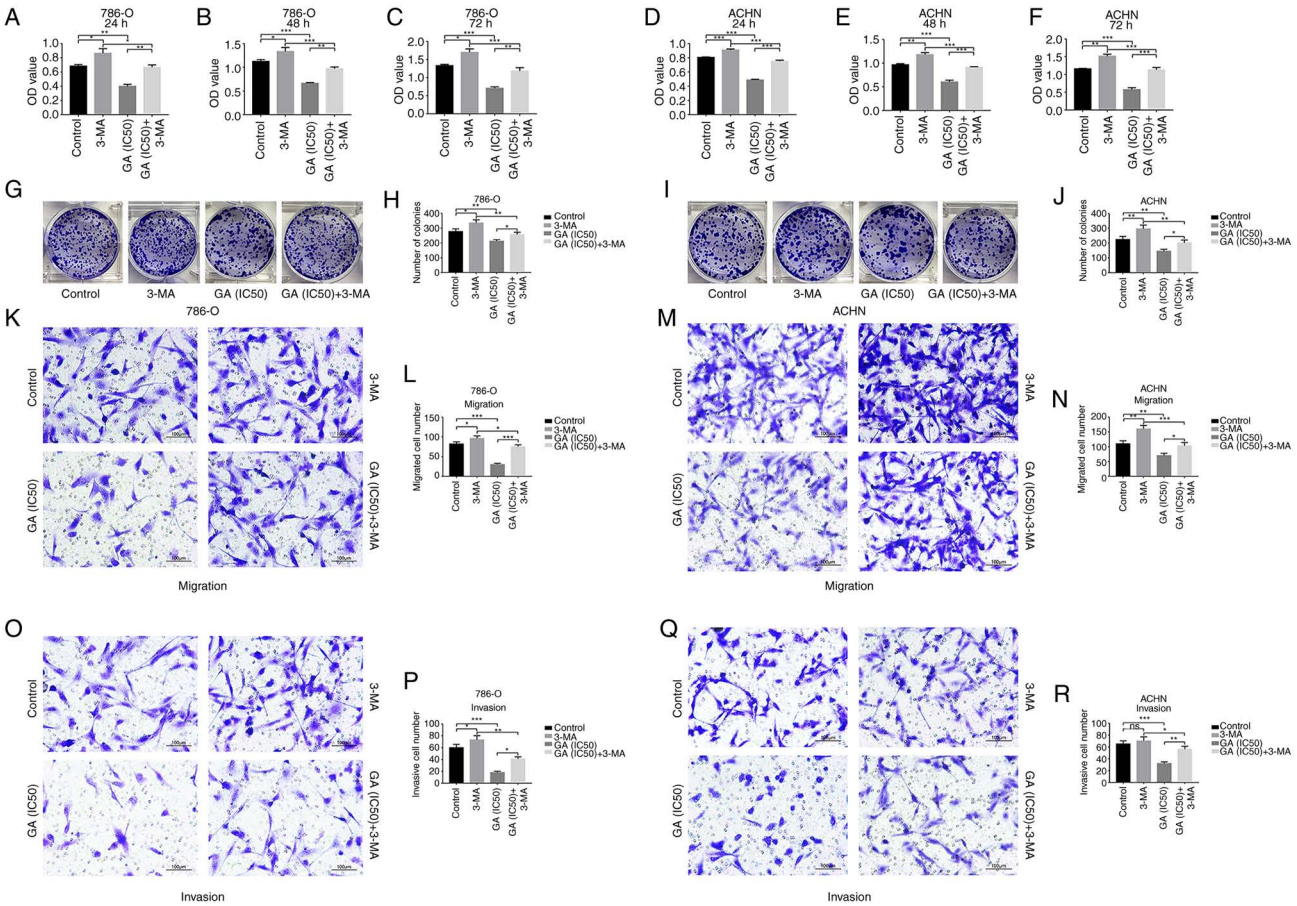

Figure 7. 3-MA reverses proliferation and metastasis of ccRCC cells inhibited by GA. (A-F) Quantitative analyses of ccRCC cells' viability in each group were measured by Cell Counting Kit-8. (G-J) Representative images and quantitative analyses of ccRCC cells' proliferation in each group were measured by the plate clone formation assay. (K-N) Representative images and quantitative analyses of ccRCC cells migration in each group were measured by the Transwell migration assay. (O-R) Representative images and quantitative analyses of ccRCC cells' invasion in each group were measured by the Matrigel invasion assay. *P<0.05, **P<0.01 and ***P<0.001 compared with the control group and GA (IC_{50}) group. 3-MA, 3-methyladenine; ccRCC, clear cell renal cell carcinoma; GA, gallic acid.

promote or inhibit cancers progression under different conditions. Therefore, the implication of autophagy in tumorigenesis remains controversial (38). Meanwhile, an increasing number of studies have shown that polyphenols can suppress the development of cancers by activating the death program of cancer cells, including autophagy. For example, Zhao *et al* (17) found

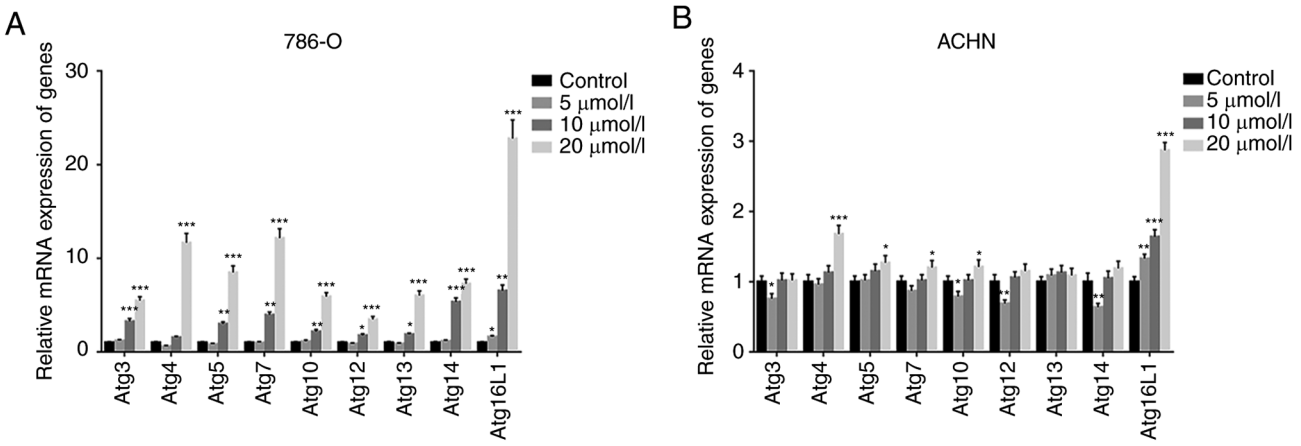

Figure 8. GA regulates the expression of Atgs in ccRCC cells. (A and B) Reverse transcription-PCR analyses of autophagy-related genes, including Atg3, Atg4, Atg5, Atg7, Atg10, Atg12, Atg13, Atg14, Atg16L1, in ccRCC cells with different concentrations of GA treatment. *P<0.05, **P<0.01 and ***P<0.001 compared with the control group. ccRCC, clear cell renal cell carcinoma; Atg, autophagy-related gene; GA, gallic acid.

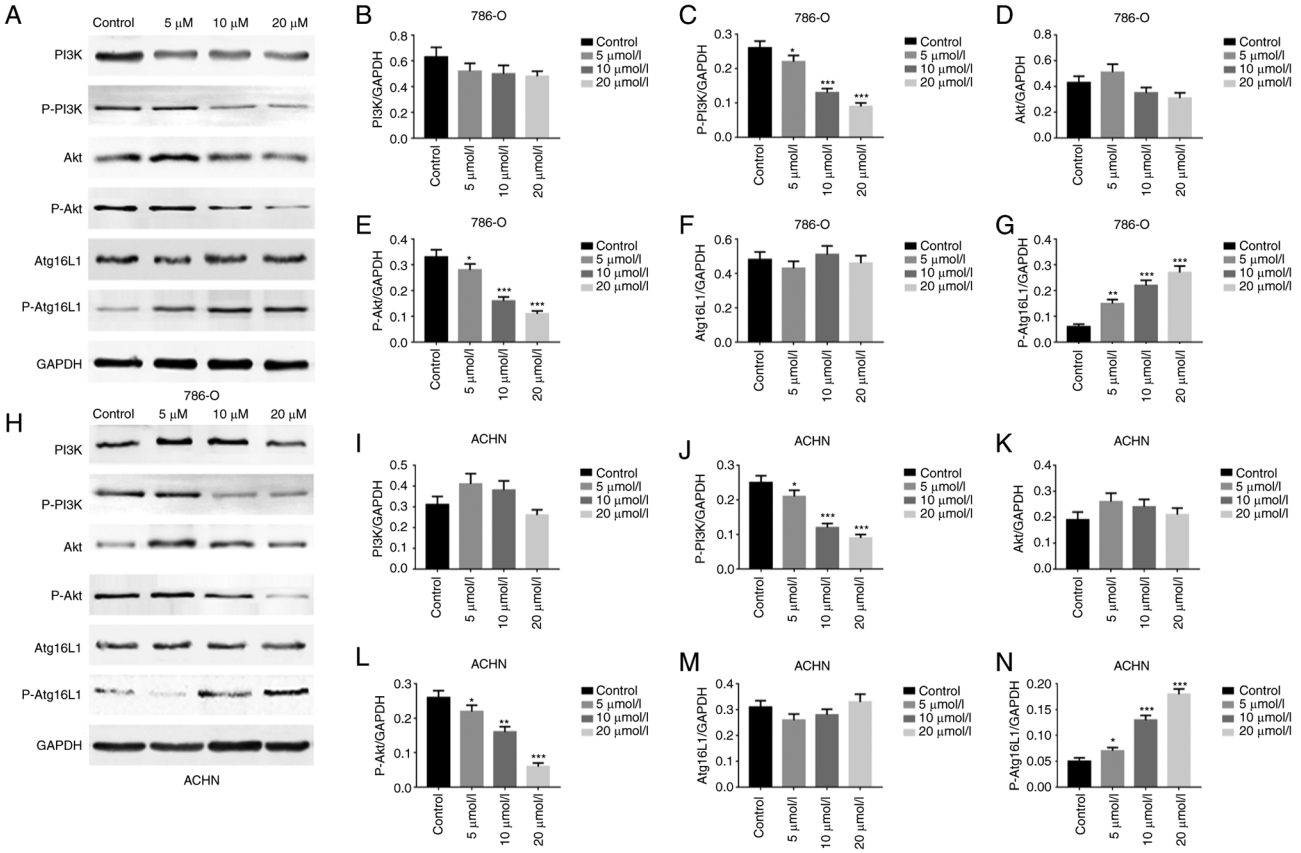

Figure 9. GA induces autophagy of ccRCC cells via the PI3K/Akt/Atg16L1 signaling pathway. (A-N) Representative western blotting images and quantitative analyses of several critical proteins, including (B and I) PI3K, (C and J) P-PI3K, (D and K) Akt, (E and L) P-Akt, (F and M) Atg16L1 and (G and N) P-Atg16L1 in ccRCC cells with different concentrations of GA treatment. GAPDH served as the internal reference. *P<0.05, **P<0.01 and ***P<0.001 compared with the control group. GA, gallic acid; ccRCC, clear cell renal cell carcinoma; P-, phosphorylated.

that urolithin A, a major polyphenol metabolite, induced both autophagy and apoptosis in colorectal cancer cells, and mainly reflected in the decreased cell proliferation, delayed cell migration and inhibited cell metastasis. Tedesco *et al* (39) indicated that the polyphenols in the lyophilized red wine induced apoptotic and autophagic cell death in human osteosarcoma in a dose-dependent manner with a maximum effect in the range of 100-200 μg/ml equivalents of GA. Liu *et al* (40) identified that *Sanguisorba officinalis* radix, a chief constituent of which is GA, inhibited colorectal cancer cell proliferation and sensitized the cancer cells to 5-FU therapy by activating a reactive oxygen species-mediated and mitochondria-caspase-dependent apoptotic pathway. Wang *et al* (19) displayed that punicalagin, a polyphenol isolated from *Punica granatum*, induced death

of human glioma cells through apoptotic and autophagic pathways, and the suppression of autophagy dose-dependently alleviated the cell death caused by punicalagin. Dong *et al* (41) demonstrated that penta-1,2,3,4,6-O-galloyl-β-D-glucose, a naturally existing gallotannin polyphenol compound found in oriental herbs, promoted senescence of cancer cells, and this process was mediated by autophagy.

However, whether GA could also inhibit the progression of ccRCC through inducing autophagy remains elusive. The present study solved this query to a certain extent. In the present study, it was firstly found that GA inhibited proliferation, migration and invasion of ccRCC cells (786-O and ACHN), with showing no or minor damage to the normal renal tubular epithelial cells (HK-2). In case of GA treatment, HK-2 cells exhibited elliptical morphology with relatively regular surfaces. During GA stimulation, there was no significant change in cell morphology with the increase of GA concentration or the extension of culture time. The vast majority of cells did not elongate into irregular shapes, and the intercellular connections remained intact. Overall, GA stimulation did not significantly destroy the morphology of HK-2 cells. To some extent, this evaluates the safety of the drug.

Moreover, GA arrested ccRCC cell cycle in S phase. The results indicated that GA could selectively inhibit ccRCC progression in a concentration-dependent manner *in vitro*. In addition, the proteins and genes' expression of autophagy markers as well as autophagosomes formation were further assessed. The results indicated that GA significantly induced autophagy of ccRCC cells. Subsequently, the nude mouse xenograft assay and the tumor metastasis assay revealed that GA significantly inhibited tumor growth and metastasis, and induced tumor autophagy in a concentration-dependent manner *in vivo*.

To further confirm the present findings, 3-MA was utilized to suppress autophagy and a remarkable reversal was observed in ccRCC cell proliferation, migration and invasion. The process of autophagy can be divided into several stages: Initiation, autophagosome formation, autophagosome maturation and lysosomal degradation. PI3K plays a crucial role in both autophagy-mediated lysosomal degradation and vesicular trafficking during the process of autophagy (42). Knocking down autophagy-related genes or blocking class III PI3-Kinase is the most common method of inhibiting autophagy.

3-MA is a classic autophagy inhibitor that exerts its inhibitory effect by blocking key steps in the formation of autophagosomes and autophagic vacuoles (43). It was initially discovered by screening purine-related substances using liver cells isolated from rats in 1982 (44). It is also considered the most extensively utilized autophagy inhibitor owing to its ability to impede the interaction between class III PI3-Kinase and several ATG partners (45). The potential value of 3-MA-mediated autophagy inhibition in tumor therapy has been demonstrated in multiple studies (46,47).

The activation of the PI3K/Akt pathway is a known causal mechanism for tumorigenesis and antitumor therapy. This is also true in the progression of RCC (48). Finally, in order to explore the specific mechanism involved in GA inducing ccRCC cells autophagy, the expression of autophagy-related genes and several critical proteins was measured, and it was found that GA induced autophagy of ccRCC cells via the PI3K/Akt/Atg16L1 signaling pathway. All these results suggested that GA could selectively inhibit proliferation, migration, and invasion of ccRCC cells as well as suppress ccRCC growth and metastasis by inducing autophagy via the PI3K/Akt/Atg16L1 signaling pathway. 3-MA acts as a pharmacological blocker of class III PI3-Kinase, preventing the formation of autophagosomes, blocking the autophagy pathway, finally reversing these effects.

Apoptosis induction is one of the targeted approaches used in cancer therapy, and serves as the primary mechanism targeted by chemotherapy drugs and polyphenols. Several natural compounds that have been previously reported to induce apoptosis have shown promising potential as candidates, as they possess the ability to regulate apoptosis through diverse signaling pathways (49,50).

Mitochondria exert critical roles in in apoptotic cell death. In a previous study by the authors, it was demonstrated that GA significantly inhibited viability of T24 bladder cancer cells in a concentration and time-dependent manner. GA induces apoptosis of T24 cells via the mitochondrial pathway. GA can inhibit T24 cells proliferation, metastasis and promote apoptosis, and the pro-apoptotic activity is closely associated with mitochondrial dysfunction and PI3K/Akt/NF-κB signaling suppression (24). In future studies, it shall be continued to explore the role of GA in apoptosis and to determine the pathway and relevant components by which GA-induced apoptosis is mediated through.

In conclusion, the present study identified that autophagy of ccRCC cells was induced in response to GA treatment. Subsequently, the *in vitro* results were translated into an animal model. The findings in cell research were consistent with those in animal study, namely, the key markers of autophagy were all observed in the *in vitro* and *in vivo* studies. Furthermore, the signaling pathway involved in GA-induced autophagy of ccRCC cells was indeed activated. Hence, it was firstly presented that GA could inhibit ccRCC progression by inducing autophagy. GA will be a promising agent, and its application may provide an effective, independent of apoptosis-resistance treatment for patients with ccRCC.

Acknowledgements

Not applicable.

Funding

The present study was supported by Anhui Medical University Basic and Clinical Cooperative Research Promotion Project (grant no. 2020xkjT031) and the National Level Innovation Training Program for Chinese College Students of the Ministry of Education of the People's Republic of China (grant no. 202110366035).

Availability of data and materials

The datasets used and/or analyzed during the current study are available from the corresponding author on reasonable request.

Authors' contributions

TZ, CZL and YS conceived and designed the present study. TZ, XZ and JL supervised and analyzed the results. YS, TZ and YF performed the experiments. LZ, DZ, JL and SF analyzed the data. YS, LZ and JZ contributed analysis tools. TZ, XZ, YS, YF and SF contributed significantly in writing the manuscript. TZ, CZL and YS confirm the authenticity of all the raw data. All authors read and approved the final version of the manuscript.

Ethics approval and consent to participate

The present study was approved (approval no. LLSC20232011) by the Ethical Committee of Anhui Medical University (Hefei, China). All applicable international, national, and/or institutional guidelines for the care and use of animals were followed.

Patient consent for publication

Not applicable.

Competing interests

The authors declare that they have no competing interests.

References

1. Petejova N and Martinek A: Renal cell carcinoma: Review of etiology, pathophysiology and risk factors. Biomed Pap Med Fac Univ Palacky Olomouc Czech Repub 160: 183-194, 2016.
2. Qu Y, Feng J, Wu X, Bai L, Xu W, Zhu L, Liu Y, Xu F, Zhang X, Yang G, *et al*: A proteogenomic analysis of clear cell renal cell carcinoma in a Chinese population. Nat Commun 13: 2052, 2022.
3. Siegel RL, Miller KD and Jemal A: Cancer statistics, 2017. CA Cancer J Clin 67: 7-30, 2017.
4. Capitanio U, Bensalah K, Bex A, Boorjian SA, Bray F, Coleman J, Gore JL, Sun M, Wood C and Russo P: Epidemiology of renal cell carcinoma. Eur Urol 75: 74-84, 2019.
5. Sun Z, Tao W, Guo X, Jing C, Zhang M, Wang Z, Kong F, Suo N, Jiang S and Wang H: Construction of a lactate-related prognostic signature for predicting prognosis, tumor microenvironment, and immune response in kidney renal clear cell carcinoma. Front Immunol 13: 818984, 2022.
6. Bi K, He MX, Bakouny Z, Kanodia A, Napolitano S, Wu J, Grimaldi G, Braun DA, Cuoco MS, Mayorga A, *et al*: Tumor and immune reprogramming during immunotherapy in advanced renal cell carcinoma. Cancer Cell 39: 649-661.e5, 2021.
7. Wolf MM, Kimryn Rathmell W and Beckermann KE: Modeling clear cell renal cell carcinoma and therapeutic implications. Oncogene 39: 3413-3426, 2020.
8. Maiuolo J, Gliozzi M, Carresi C, Musolino V, Oppedisano F, Scarano F, Nucera S, Scicchitano M, Bosco F, Macri R, *et al*: Nutraceuticals and cancer: Potential for natural polyphenols. Nutrients 13: 3834, 2021.
9. Zhao B and Hu M: Gallic acid reduces cell viability, proliferation, invasion and angiogenesis in human cervical cancer cells. Oncol Lett 6: 1749-1755, 2013.
10. Tuli HS, Mistry H, Kaur G, Aggarwal D, Garg VK, Mittal S, Yerer MB, Sak K and Khan MA: Gallic acid: A dietary polyphenol that exhibits anti-neoplastic activities by modulating multiple oncogenic targets. Anticancer Agents Med Chem 22: 499-514, 2022.
11. Al Zahrani NA, El-Shishtawy RM and Asiri AM: Recent developments of gallic acid derivatives and their hybrids in medicinal chemistry: A review. Eur J Med Chem 204: 112609, 2020.
12. Bai J, Zhang Y, Tang C, Hou Y, Ai X, Chen X, Zhang Y, Wang X and Meng X: Gallic acid: Pharmacological activities and molecular mechanisms involved in inflammation-related diseases. Biomed Pharmacother 133: 110985, 2021.
13. Ashrafizadeh M, Zarrabi A, Mirzaei S, Hashemi F, Samarghandian S, Zabolian A, Hushmandi K, Ang HL, Sethi G, Kumar AP, *et al*: Gallic acid for cancer therapy: Molecular mechanisms and boosting efficacy by nanoscopical delivery. Food Chem Toxicol 157: 112576, 2021.
14. Deng B, Yang B, Chen J, Wang S, Zhang W, Guo Y, Han Y, Li H, Dang Y, Yuan Y, *et al*: Gallic acid induces T-helper-1-like T_{reg} cells and strengthens immune checkpoint blockade efficacy. J Immunother Cancer 10: e004037, 2022.
15. Zhang HH, Zhang Y, Cheng YN, Gong FL, Cao ZQ, Yu LG and Guo XL: Metformin incombination with curcumin inhibits the growth, metastasis, and angiogenesis of hepatocellular carcinoma in vitro and in vivo. Mol Carcinog 57: 44-56, 2018.
16. Lin Y, Luo T, Weng A, Huang X, Yao Y, Fu Z, Li Y, Liu A, Li X, Chen D and Pan H: Gallic acid alleviates gouty arthritis by inhibiting NLRP3 inflammasome activation and pyroptosis through enhancing Nrf2 signaling. Front Immunol 11: 580593, 2020.
17. Zhao W, Shi F, Guo Z, Zhao J, Song X and Yang H: Metabolite of ellagitannins, urolithin A induces autophagy and inhibits metastasis in human sw620 colorectal cancer cells. Mol Carcinog 57: 193-200, 2018.
18. Cao Y, Chen J, Ren G, Zhang Y, Tan X and Yang L: Punicalagin prevents inflammation in LPS-induced RAW264.7 macrophages by inhibiting FoxO3a/autophagy signaling pathway. Nutrients 11: 2794, 2019.
19. Wang SG, Huang MH, Li JH, Lai FI, Lee HM and Hsu YN: Punicalagin induces apoptotic and autophagic cell death in human U87MG glioma cells. Acta Pharmacol Sin 34: 1411-1419, 2013.
20. Klionsky DJ, Petroni G, Amaravadi RK, Baehrecke EH, Ballabio A, Boya P, Bravo-San Pedro JM, Cadwell K, Cecconi F, Choi AMK, *et al*: Autophagy in major human diseases. EMBO J 40: e108863, 2021.
21. Ferro F, Servais S, Besson P, Roger S, Dumas JF and Brisson L: Autophagy and mitophagy in cancer metabolic remodelling. Semin Cell Dev Biol 98: 129-138, 2020.
22. Moon S and Jung HS: Endoplasmic reticulum stress and dysregulated autophagy in human pancreatic beta cells. Diabetes Metab J 46: 533-542, 2022.
23. Li X, He S and Ma B: Autophagy and autophagy-related proteins in cancer. Mol Cancer 19: 12, 2020.
24. Zeng M, Su Y, Li K, Jin D, Li Q, Li Y and Zhou B: Gallic acid inhibits bladder cancer T24 cell progression through mitochondrial dysfunction and PI3K/Akt/NF-κB signaling suppression. Front Pharmacol 11: 1222, 2020.
25. Khadirnaikar S, Kumar P, Pandi SN, Malik R, Dhanasekaran SM and Shukla SK: Immune associated LncRNAs identify novel prognostic subtypes of renal clear cell carcinoma. Mol Carcinog 58: 544-553, 2019.
26. Sales MS, Roy A, Antony L, Banu SK, Jeyaraman S and Manikkam R: Octyl gallate and gallic acid isolated from Terminalia bellarica regulates normal cell cycle in human breast cancer cell lines. Biomed Pharmacother 103: 1577-1584, 2018.
27. Gu R, Zhang M, Meng H, Xu D and Xie Y: Gallic acid targets acute myeloid leukemia via Akt/mTOR-dependent mitochondrial respiration inhibition. Biomed Pharmacother 105: 491-497, 2018.
28. Pham HNT, Sakoff JA, Vuong QV, Bowyer MC and Scarlett CJ: Comparative cytotoxic activity between kaempferol and gallic acid against various cancer cell lines. Data Brief 21: 1033-1036, 2018.
29. Rosman R, Saifullah B, Maniam S, Dorniani D, Hussein MZ and Fakurazi S: Improved anticancer effect of magnetite nanocomposite formulation of GALLIC Acid (Fe_3O_4-PEG-GA) against lung, breast and colon cancer cells. Nanomaterials (Basel) 8: 83, 2018.
30. Hong Z, Tang P, Liu B, Ran C, Yuan C, Zhang Y, Lu Y, Duan X, Yang Y and Wu H: Ferroptosis-related genes for overall survival prediction in patients with colorectal cancer can be inhibited by gallic acid. Int J Biol Sci 17: 942-956, 2021.
31. Cai L, Wei Z, Zhao X, Li Y, Li X and Jiang X: Gallic acid mitigates LPS-induced inflammatory response via suppressing NF-κB signalling pathway in IPEC-J2 cells. J Anim Physiol Anim Nutr (Berl) 106: 1000-1008, 2022.
32. Zhang P, Ye J, Dai J, Wang Y, Chen G, Hu J, Hu Q and Fei J: Gallic acid inhibits osteoclastogenesis and prevents ovariectomy-induced bone loss. Front Endocrinol (Lausanne) 13: 963237, 2022.
33. Lee HL, Lin CS, Kao SH and Chou MC: Gallic acid induces G1 phase arrest and apoptosis of triple-negative breast cancer cell MDA-MB-231 via p38 mitogen-activated protein kinase/p21/p27 axis. Anticancer Drugs 28: 1150-1156, 2017.

34. Lima KG, Krause GC, Schuster AD, Catarina AV, Basso BS, De Mesquita FC, Pedrazza L, Marczak ES, Martha BA, Nunes FB, *et al*: Gallic acid reduces cell growth by induction of apoptosis and reduction of IL-8 in HepG2 cells. Biomed Pharmacother 84: 1282-1290, 2016.
35. Ho HH, Chang CS, Ho WC, Liao SY, Lin WL and Wang CJ: Gallic acid inhibits gastric cancer cells metastasis and invasive growth via increased expression of RhoB, downregulation of AKT/small GTPase signals and inhibition of NF-κB activity. Toxicol Appl Pharmacol 266: 76-85, 2013.
36. Subramanian AP, Jaganathan SK, Mandal M, Supriyanto E and Muhamad II: Gallic acid induced apoptotic events in HCT-15 colon cancer cells. World J Gastroenterol 22: 3952-3961, 2016.
37. Boya P, Reggiori F and Codogno P: Emerging regulation and functions of autophagy. Nat Cell Biol 15: 713-720, 2013.
38. Das S, Shukla N, Singh SS, Kushwaha S and Shrivastava R: Mechanism of interaction between autophagy and apoptosis in cancer. Apoptosis 26: 512-533, 2021.
39. Tedesco I, Russo M, Bilotto S, Spagnuolo C, Scognamiglio A, Palumbo R, Nappo A, Iacomino G, Moio L and Russo GL: Dealcoholated red wine induces autophagic and apoptotic cell death in an osteosarcoma cell line. Food Chem Toxicol 60: 377-384, 2013.
40. Liu MP, Liao M, Dai C, Chen JF, Yang CJ, Liu M, Chen ZG and Yao MC: Sanguisorba officinalis L synergistically enhanced 5-fluorouracil cytotoxicity in colorectal cancer cells by promoting a reactive oxygen species-mediated, mitochondria-caspase-dependent apoptotic pathway. Sci Rep 6: 34245, 2016.
41. Dong Y, Yin S, Jiang C, Luo X, Guo X, Zhao C, Fan L, Meng Y, Lu J, Song X, *et al*: Involvement of autophagy induction in penta-1, 2,3,4,6-O-galloyl-β-D-glucose-induced senescence-like growth arrest in human cancer cells. Autophagy 10: 296-310, 2014.
42. Iershov A, Nemazanyy I, Alkhoury C, Girard M, Barth E, Cagnard N, Montagner A, Chretien D, Rugarli EI, Guillou H, *et al*: The class 3 PI3K coordinates autophagy and mitochondrial lipid catabolism by controlling nuclear receptor PPARα. Nat Commun 10: 1566, 2019.
43. Zhao F, Feng G, Zhu J, Su Z, Guo R, Liu J, Zhang H and Zhai Y: 3-Methyladenine-enhanced susceptibility to sorafenib in hepatocellular carcinoma cells by inhibiting autophagy. Anticancer Drugs 32: 386-393, 2021.
44. Seglen PO and Gordon PB: 3-Methyladenine: Specific inhibitor of autophagic/lysosomal protein degradation in isolated rat hepatocytes. Proc Natl Acad Sci USA 79: 1889-1892, 1982.
45. Vinod V, Padmakrishnan CJ, Vijayan B and Gopala S: 'How can I halt thee?' The puzzles involved in autophagic inhibition. Pharmacol Res 82: 1-8, 2014.
46. Li J, Hou N, Faried A, Tsutsumi S, Takeuchi T and Kuwano H: Inhibition of autophagy by 3-MA enhances the effect of 5-FU-induced apoptosis in colon cancer cells. Ann Surg Oncol 16: 761-771, 2009.
47. Li J, Yang D, Wang W, Piao S, Zhou J, Saiyin W, Zheng C, Sun H and Li Y: Inhibition of autophagy by 3-MA enhances IL-24-induced apoptosis in human oral squamous cell carcinoma cells. J Exp Clin Cancer Res 34: 97, 2015.
48. Guo H, German P, Bai S, Barnes S, Guo W, Qi X, Lou H, Liang J, Jonasch E, Mills GB and Ding Z: The PI3K/AKT pathway and renal cell carcinoma. J Genet Genomics 42: 343-353, 2015.
49. Rajabi S, Maresca M, Yumashev AV, Choopani R and Hajimehdipoor H: The most competent plant-derived natural products for targeting apoptosis in cancer therapy. Biomolecules 11: 534, 2021.
50. Chimento A, De Luca A, D'Amico M, De Amicis F and Pezzi V: The involvement of natural polyphenols in molecular mechanisms inducing apoptosis in tumor cells: A promising adjuvant in cancer therapy. Int J Mol Sci 24: 1680, 2023.